

# Electron Relaxation in Silicon Quantum Dots by Acoustic Phonon Scattering

M. Dür, A. D. Gunther, D. Vasileska, and S. M. Goodnick

Department of Electrical Engineering  
Arizona State University, Tempe, AZ 85287-5706, USA  
Phone: +1-602-965-2030, Fax: +1-602-965-3837  
E-mail: duer@asu.edu

Acoustic phonon scattering of electrons in fully quantized systems based on  $n$ -type inversion layers on a (100) surface of  $p$ -type Si is studied theoretically. The confining potential normal to the Si/SiO<sub>2</sub> interface is modeled by a triangular quantum well. For the confinement in the lateral directions we assume a parabolic potential. The calculations reveal that the anisotropic electron-phonon interaction strongly affects the scattering rate. The calculated transition rate of electrons from the first excited to the ground state shows a strong dependence on spatial confinement and lattice temperature.

## 1. Introduction

In recent years, there has been considerable interest in the study of electron relaxation in quantum dots by means of acoustic phonon scattering [1-3]. However, most of the theoretical work thus far has been devoted to quantum dots in GaAs, whereas relatively little has been reported concerning Si quantum dots. In Si, electron-phonon scattering tends to be more complicated because of its multivalley bandstructure and ellipsoidal energy surfaces. Here we report on acoustic phonon scattering in quantum dots based on the Si MOS technology.

The device we consider in this work was fabricated recently [4] and consists of a MOS structure with  $n$ -type inversion layer on a (100) surface of  $p$ -type Si [5]. When a positive voltage is applied to the top gate, electrons accumulate in the inversion layer near the Si/SiO<sub>2</sub> interface. Because of the strong surface electric field, the motion of electrons is quantized normal to the interface but unconstrained in the plane parallel to the interface. Additional confinement in the lateral directions is achieved with depletion gates close to the interface. When a negative voltage is applied to these gates, the electrons are repelled and cannot accumulate underneath them. Consequently, the electrons are confined to a very small region (typically on the order of 200 nm × 200 nm) between the depletion gates which leads to the formation of a quantum dot with a completely discrete energy spectrum.

## 2. Physical model

### Energies and Wave Functions

We model the spatial confinement of electrons in the

direction normal to the Si/SiO<sub>2</sub> interface, taken as the  $z$  axis, by an infinite triangular quantum well. For the lateral confinement, we assume a parabolic form of the potential. Then the effective-mass Hamiltonian of the quantum dot system embedded in a (100) inversion layer can be written as

$$H = H_{xy} + H_z. \quad (1)$$

The motion of electrons along the  $z$  axis is decoupled from the lateral motion and the envelope wave functions separate,  $\psi(\mathbf{r}) = \phi(x, y)\xi(z)$ . The  $z$ -dependent part  $\xi$  is an eigenfunction of the triangular quantum well Hamiltonian

$$H_z = \frac{p_z^2}{2m_z} + \begin{cases} eFz & : z \geq 0 \\ \infty & : z < 0 \end{cases}, \quad (2)$$

where  $m_z$  is the effective mass along the  $z$  direction and  $F$  is the effective electric field in the inversion layer. The Schrödinger equation corresponding to  $H_z$  is solved with the condition that the eigenfunctions vanish for  $z = 0$  and  $z \rightarrow \infty$ . The solutions  $\xi_{n_z}$  are given by Airy functions, where  $n_z = 0, 1, 2, \dots$  denotes the subband index.

For a (100) surface orientation, the six equivalent valleys along the  $\Delta$  axes in the Brillouin zone of Si give two ladders of subband minima  $E_{n_z}$ , depending on the value of  $m_z$  in Eq. (2). The unprimed ladder originates from the heavy, longitudinal mass  $m_l = 0.916m_0$  of the ellipsoidal constant-energy surface, while the primed ladder arises from the light, transverse mass  $m_t = 0.19m_0$ .

In Figure 1, the subband energies and average distance of electrons from the Si/SiO<sub>2</sub> interface are

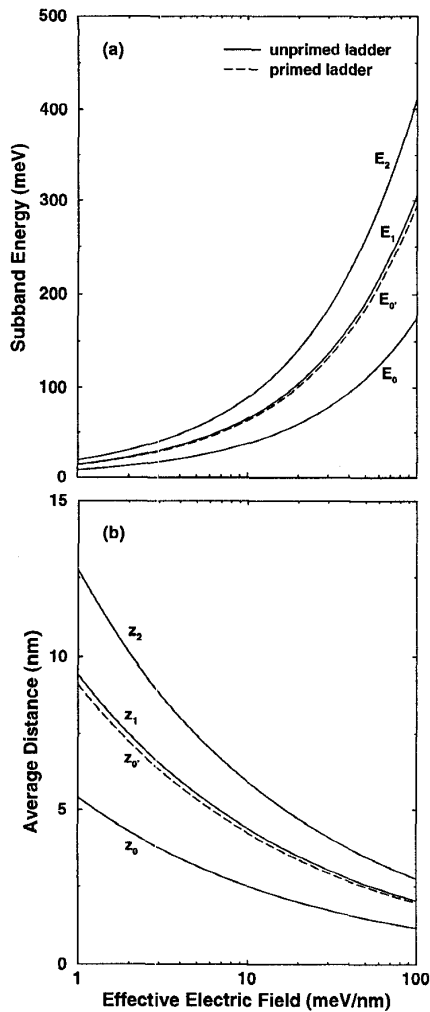


Figure 1: Subband minima (a) and average distance of electrons from the interface (b) versus effective electric field in the inversion layer.

shown as a function of the effective electric field for both subband ladders. Since the unprimed ladder presents the highest mass for motion perpendicular to the surface, it has the lowest kinetic energy and thus the lowest lying energy level. The average distance of electrons in the  $n_z$ th subband from the interface  $z_{n_z}$  is given by  $2E_{n_z}/(3eF)$  [5]. As the effective field seen by the electrons in the inversion layer increases, the confinement becomes stronger. For this reason, the average spatial extent of electrons from the interface decreases and the subband minima as well as their separation shift to higher energies.

The electronic motion along the lateral directions is

described by the Hamiltonian

$$H_{xy} = \frac{p_x^2}{2m_x} + \frac{p_y^2}{2m_y} + \frac{1}{2}(K_x x^2 + K_y y^2), \quad (3)$$

where  $m_x$  and  $m_y$  are the lateral effective masses.  $K_x$  and  $K_y$  characterize the strength of the parabolic confinement. The bound states  $\phi_{n_x n_y}$  are products of one-dimensional harmonic oscillator states  $n_x$  and  $n_y$  ( $n_x, n_y = 0, 1, 2, \dots$ ) with energies  $\hbar\omega_x$  and  $\hbar\omega_y$ . The characteristic frequencies  $\omega_x$  and  $\omega_y$  of the lateral confinement are related with  $K_x$  and  $K_y$  in (3) by  $\omega_x = \sqrt{K_x/m_x}$  and  $\omega_y = \sqrt{K_y/m_y}$ . Therefore, the electronic spectrum of the quantum dot system may be labeled by a triple of integers  $(n_x, n_y, n_z)$ .

### Acoustic Phonon Scattering

The interaction of electrons in the dot with bulk-like acoustic phonons in Si is treated within the deformation potential theory [6]. For intervalley transitions, we assume constant deformation potentials, whereas for intravalley transitions, the angular dependence of the deformation potentials is included in the interaction Hamiltonian [7],

$$H_{ac}(\mathbf{r}) = \Xi_d[\epsilon_{xx}(\mathbf{r}) + \epsilon_{yy}(\mathbf{r}) + \epsilon_{zz}(\mathbf{r})] + \Xi_u \epsilon_{zz}(\mathbf{r}). \quad (4)$$

$\epsilon_{xx}$ ,  $\epsilon_{yy}$ , and  $\epsilon_{zz}$  denote the components of the strain tensor in a coordinate system formed by the principal axes of a given ellipsoidal valley in Si, and  $\Xi_d$  and  $\Xi_u$  are the dilatation and uniaxial-shear deformation potentials, respectively. Employing an isotropic phonon dispersion for both the longitudinal (LA) and transverse (TA) acoustic modes, the transition rate for electron scattering between energy levels in the dot is calculated from the Fermi golden rule.

### 3. Results and Discussion

In the following, we present results for the ground subband  $n_z = 0$  of the unprimed ladder of subbands with  $m_z = m_l$  and  $m_x = m_y = m_t$ , assuming isotropic lateral confinement.

Figure 2 shows the transition rate for electron scattering from the first excited state to the ground state as a function of lateral confinement energy divided into contributions from longitudinal and transverse phonon modes. The rate is plotted for two different sets of deformation potential constants ( $\Xi_d$ ,  $\Xi_u$ ) used in studies of electron transport in Si (set I:  $\Xi_d = 1.13$  eV,  $\Xi_u = 9.16$  eV [8]; set II:  $\Xi_d = -11.7$  eV,  $\Xi_u = 9.0$  eV [9]). The calculations are made for an effective electric field  $eF = 10$  meV/nm at a lattice temperature  $T = 0$  K. As a consequence of the anisotropic electron-phonon interaction, the scattering rate is very sensitive to the choice of deformation potentials, as discussed in detail elsewhere [10]. For both choices of deformation potential constants, the transition rates first increase with lateral confinement energy, reach a maximum and then fall off for large confinement energies. Except for small confinement energies, the main

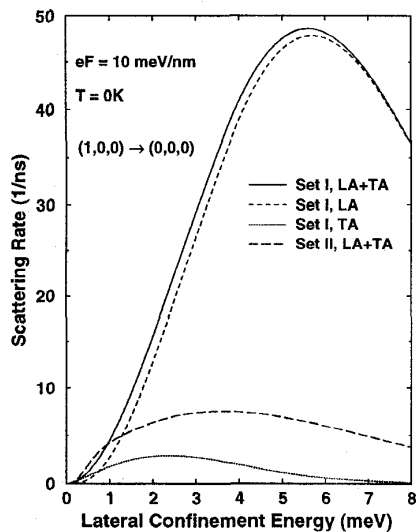


Figure 2: Scattering rate from the first excited to the ground state versus lateral confinement energy.

contribution to the total rate comes from the longitudinal mode which has a smaller wave vector involved in a transition. This smaller wave vector is associated with larger values of the form factors included in the scattering matrix element.

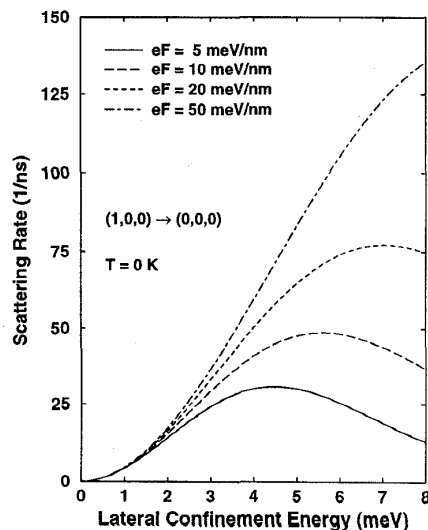


Figure 3: Scattering rate versus lateral confinement for different effective fields in the inversion layer.

Figure 3 shows the effect on the scattering rate for different effective fields in the inversion layer or, equivalently, how the spatial confinement of electrons in the  $z$  direction affects the scattering. Since a higher effective field causes stronger localization of the wave function

along the  $z$  axis (For  $eF = 5$  meV/nm, the average distance of electrons from the interface  $z_0$  is 5.4 nm. For  $eF = 50$  meV/nm,  $z_0$  drops to 1.4 nm), the respective form factor is more spread out in momentum space. Therefore, the overlap between the form factors in all directions increases, thereby enhancing the scattering rate.

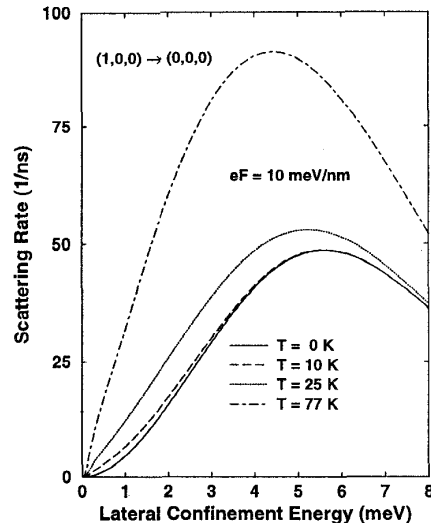


Figure 4: Scattering rate versus lateral confinement for different lattice temperatures.

Figure 4 shows the scattering rate versus confinement for four different lattice temperatures. Since the emission rate is proportional to  $n_B + 1$ , where  $n_B$  is the phonon occupation number, the rate strongly increases with with temperature for confinement energies smaller than the thermal energy of the lattice. For sufficiently large phonon energies involved in the transition, the occupation number goes to zero and all curves merge.

#### 4. Conclusions

In summary, we have presented a theoretical study of electron scattering by acoustic phonons in Si quantum dots embedded in a MOS structure. Our results reveal that the anisotropic electron-phonon interaction strongly affects the scattering rate. We find that the decay of electrons from the first excited level into the ground level of the dot shows a strong influence of spatial confinement and lattice temperature on the calculated emission rates, with the main contribution coming from the longitudinal phonon mode.

#### Acknowledgments

This work was partially supported by the Office of Naval Research, Grant No. N00014-93-1-0618. Additionally, one of us (M.D.) would also like to acknowledge the support of the Austrian Science Foundation through the Schrödinger Fellowship in this work.

## References

1. U. Bockelmann, Phys. Rev. B **50**, 17 271 (1994).
2. H. Benisty, Phys. Rev. B **51**, 13 281 (1995).
3. T. Inoshita and H. Sakaki, Phys. Rev. B **46**, 7260 (1992).
4. M. Khoury, D. P. Pivin, M. J. Rack, A. Gunther, and D. K. Ferry, Nanotechnology, in press.
5. T. Ando, A. B. Fowler, and F. Stern, Rev. Mod. Phys. **54**, 437 (1982).
6. G. L. Bir and G. E. Pikus, *Symmetry and Strain-Induced Effects in Semiconductors* (Wiley & Sons, New York, 1974).
7. C. Herring and E. Vogt, Phys. Rev. **101**, 944 (1956).
8. C. G. van de Walle, Phys. Rev. B **39**, 1871 (1989); M. V. Fischetti and S. E. Laux, J. Appl. Phys. **80**, 2234 (1996).
9. M. V. Fischetti and S. E. Laux, Phys. Rev. B **48**, 2244 (1993).
10. M. Dür, A. D. Gunther, D. Vasileska, and S. M. Goodnick, Nanotechnology, in press.